Photocatalytic Activity Enhancing for Titanium Dioxide by Co-doping with Bromine and Chlorine

Hongmei Luo,[†] Tsuyoshi Takata,[‡] Yungi Lee,[‡] Jinfeng Zhao,[†] Kazunari Domen,[‡] and Yushan Yan*,[†]

Department of Chemical and Environmental Engineering, University of California, Riverside, California 92521, and Chemical Resources Laboratory, Tokyo Institute of Technology, Nagatsuta 4259, Midori-Ku, Yokohama 226-8503, Japan

Received October 30, 2003. Revised Manuscript Received December 21, 2003

Bromine and chlorine co-doped nanocrystalline titanium dioxide are synthesized by a hydrothermal method using titanium chloride in a mixed hydrobromic acid−ethanol system. TiO_2 with anatase, mixed anatase/rutile, rutile, mixed rutile/brookite, mixed anatase/rutile/brookite, and rutile phases are obtained, in that order, by increasing the acidity through addition of HBr. Br^- and Cl^- co-doping causes the absorption edge of TiO_2 to shift to a lower energy region. The photocatalytic activity of doped TiO_2 with mixed anatase/rutile phases exceeds that of commercial TiO_2 photocatalyst Degussa P-25 for water splitting into H_2 and O_2 under ultraviolet light.

1. Introduction

Water splitting into H_2 and O_2 using semiconductor photocatalysts could be an ideal route to renewable hydrogen generation with great potential for future energy and the environment.[1,2] Titanium dioxide (TiO_2) has been used widely as a photocatalyst due to its optical and electronic properties, long-term stability, low cost, and nontoxicity. With a band gap of 3.0−3.3 eV, TiO_2 has become photocatalytically active only under ultraviolet (UV) light (wavelength λ < 400 nm). However, it is desirable to develop a photocatalyst that efficiently absorbs visible light, which occupies the main part of the solar spectrum. Doping of various transition metal ions or rare earth ions in TiO_2 have been intensively investigated for photocatalytic decomposition of organic compounds.[3−6] Very recently, Asahi et al. reported that nitrogen (N) doping in TiO_2 shifted its optical absorption and enhanced the photocatalytic activity such as photodegradation of methylene blue and gaseous acetaldehyde in the visible region of λ < 500 nm.[7] Titanium (Ti)-, Niobium (Nb)-, or Tantalum (Ta)-based oxynitrides were recently studied as new photocatalysts for water splitting under visible light irradiation.[8] Khan et al. reported that substitution of carbon (C) for oxygen in TiO_2 lowered its band gap to absorb visible light and $TiO_{2-x}C_x$ had higher photocurrent density and photoconversion efficiency for water splitting.[9] Fluorine (F) doping caused red shift in the absorption edge and F-doped TiO_2 showed higher activity on the photocatalytic oxidation of acetone under UV light.[10,11] Co-doping of N and F in TiO_2 to $TiO_xN_yF_z$ had a band-gap absorption edge at 570 nm and was shown to be effective for water oxidation.[12] Sulfur (S) doping was reported to narrow the band gap of TiO_2,[13] and Ti-based oxysulfide $Sm_2Ti_2S_2O_5$ was found as a visible light-driven photocatalyst for water splitting.[14]

It is clear that N, C, F, and S-doping for oxygen in TiO_2 could narrow the band gap, possibly leading to new visible light-driven photocatalysts. In this study, we incorporated bromine (Br^-) and chlorine (Cl^-) into TiO_2 by hydrothermal synthesis using titanium chloride ($TiCl_4$) as the titanium source in a mixed hydrobromic acid (HBr, 48%)−ethanol solution. With an increase of HBr amount in the solution, pure anatase, mixed anatase/rutile, pure rutile, mixed rutile/brookite, and mixed anatase/rutile/brookite phases were obtained. Co-

* To whom correspondence should be addressed. E-mail: yushan.yan@ucr.edu.
[†] University of California.
[‡] Tokyo Institute of Technology.

(1) Fujishima, A.; Honda, K. *Nature* **1972**, *238*, 37.
(2) Review, see Mills, A.; Hunte, S. L. *J. Photochem. Photobiol. A* **1997**, *108*, 1. Takata, T.; Tanaka, A.; Hara, M.; Kondo, J. N.; Domen, K. *Catal. Today* **1998**, *44*, 17. Domen, K.; Kondo, J. N.; Hara, M.; Takata, T. *Bull. Chem. Soc. Jpn.* **2000**, *73*, 1307.
(3) Choi, W.; Termin, A.; Hoffmann, M. R. *J. Phys. Chem.* **1994**, *98*, 13669.
(4) Di Paola, A.; García-López, E.; Ikeda, S.; Marcì, G.; Ohtani, B.; Palmisano, L. *Catal. Today* **2002**, *75*, 87.
(5) Xu, A.-W.; Gao, Y.; Liu, H.-Q. *J. Catal.* **2002**, *207*, 151.
(6) Kato, H.; Kudo, A. *J. Phys. Chem. B* **2002**, *106*, 5029.
(7) Asahi, R.; Morikawa, T.; Ohwaki, T.; Aoki, K.; Taga, Y. *Science* **2001**, *293*, 269.
(8) Hitoki, G.; Takata, T.; Kondo, J. N.; Hara, M.; Kobayashi, H.; Domen, K. *Electrochemistry* **2002**, *70*, 463. Kasahara, A.; Nukumizu, K.; Takata, T.; Kondo, J. N.; Hara, M.; Kobayashi, H.; Domen, K. *J. Phys. Chem. B* **2003**, *107*, 791. Kasahara, A.; Nukumizu, K.; Hitoki, G.; Takata, T.; Kondo, J. N.; Hara, M.; Kobayashi, H.; Domen, K. *Chem. Commun.* **2002**, *16*, 1698. Hitoki, G.; Takata, T.; Kondo, J. N.; Hara, M.; Kobayashi, H.; Domen, K. *J. Phys. Chem. A* **2002**, *106*, 6750. Hitoki, G.; Ishikawa, A.; Takata, T.; Kondo, J. N.; Hara, M.; Domen, K. *Chem. Lett.* **2002**, *7*, 736.
(9) Khan, S. U. M.; Al-Shahry, M.; Ingler, W. B., Jr. *Science* **2002**, *297*, 2243.
(10) Yu, J. C.; Yu, J.; Ho, W.; Jiang, Z.; Zhang, L. *Chem. Mater.* **2002**, *14*, 3808.
(11) Hattori, A.; Tada, H. *J. Sol-Gel Sci. Technol.* **2001**, *22*, 47.
(12) Nukumizu, K.; Nunoshige, J.; Takata, T.; Kondo, J. N.; Hara, M.; Kobayashi, H.; Domen, K. *Chem. Lett.* **2003**, *32*, 196.
(13) Umebayashi, T.; Yamaki, T.; Itoh, H.; Asai, K. *Appl. Phys. Lett.* **2002**, *81*, 454.
(14) Ishikawa, A.; Takata, T.; Kondo, J. N.; Hara, M.; Kobayashi, H.; Domen, K. *J. Am. Chem. Soc.* **2002**, *124*, 13547.

10.1021/cm035090w CCC: $27.50
Published on Web 01/30/2004

Table 1. Synthetic Conditions, Phase Content, Crystallite Size, Dopant Content, Surface Area, and Band Gap of Br and Cl Co-doped TiO_2[a]

				EDX (at. %)			
sample	HBr (mL)	phase	crystallite size[c] (nm)	Cl	Br	surface area (m^2/g)	band gap (eV)
A	0	A	6.5	2.7	0	174	2.95
B	3	A	6.5	2.6	0.5	161	3.0
C	5	A(70%) + R(30%)	6.0(A)	1.7	1.2	174	2.95
D	10	R	6.0	0.9	1.8	109	2.85
E	20	R(60%) + B(40%)	7.0(B)	0.8	1.7	115	
F[b]	31	A(46%) + R(12%) + B(42%)	6.0(B)	1.1	1.2	126	
G[b]	35	R	4	0.6	0.9	49	
P-25		A(80%) + R(20%)		0.01−0.3[d]	50		

[a] Doped TiO_2 was prepared by 2 mL of $TiCl_4$ + 30 mL of ethanol + HBr by a hydrothermal method at 100 °C for 1 day [b] Samples F and G were prepared by 2 mL of $TiCl_4$ + 10 mL of ethanol + HBr by a hydrothermal method at 100 °C for 1 day [c] Calculated by applying the Scherrer formula on the anatase (101), rutile (110), or brookite (121) diffraction peak. A for anatase, R for rutile, and B for brookite. [d] See refs 23 and 24.

doping of Br^- and Cl^- into the lattice of TiO_2 was shown to contribute to the band gap narrowing and enhance the photocatalytic activity for water splitting into H_2 and O_2 in Na_2CO_3 aqueous solution under UV light.

2. Experimental Section

2.1. Preparation. Titanium chloride ($TiCl_4$) and hydrobromic acid (HBr) were purchased from Alfa Aesar, and ethanol was purchased from Aldrich. All chemicals were used as received. TiO_2 particles were prepared by adding 2 mL of $TiCl_4$ to stainless steel autoclaves with Teflon liner containing mixed solutions of 30 mL of ethanol and 0−31 mL of HBr. After being sealed, the autoclaves were heated in a convection oven at 100 °C for 1 day. The products were collected by filtration, washed by ethanol several times until no Cl^- and Br^- were left in the solution as tested by silver nitrate ($AgNO_3$). The samples were then dried at 60 °C before characterization.

2.2. Characterization. The X-ray diffraction (XRD) patterns were obtained on a Siemens D-500 diffractometer using Cu Kα radiation. Scanning electron microscopy (SEM) images were obtained in a Philips XL30-FEG equipped with an energy-dispersive X-ray (EDX) spectrometer and operated at 20 kV. Nitrogen adsorption−desorption measurements were carried out at 77 K on a Micromeritics ASAP 2010 instrument to determine the Brunauer−Emmett−Teller (BET) surface area. Before measurement, samples were evacuated overnight at 100 °C and 1 μTorr. The optical absorption is represented by the Kubelka−Munk function calculated from the diffuse reflectance spectra (DRS).[15] The photocatalytic water splitting reaction was performed using a glass-made closed gas-circulating system with an inner-irradiation quartz reactor.[16,17] The light source was a 450-W high-pressure Hg lamp covered with a water-cooled quartz jacket. The reaction mixture was prepared by introduction of TiO_2 (0.3 g), H_2PtCl_6 (Pt 0.3 wt % to TiO_2), and Na_2CO_3 (92.3 g) in distilled water (400 mL) in the quartz reactor. The catalyst Pt was loaded on TiO_2 by in situ photochemical deposition from H_2PtCl_6 under irradiation.[18] The reaction mixture was mixed well using a magnetic stirrer and deaerated thoroughly. After irradiation for 15 h, the first run started. The amounts of H_2 and O_2 were determined using on-line gas chromatography. Photocatalytic activity tests were repeated three times and average data were reported. For comparison, the photocatalytic activity of the standard Degussa P-25 TiO_2 was also examined in the same system under the same conditions.

3. Results and Discussion

3.1. Effects of Acidity on the Synthesis of Titania. Table 1 shows the synthetic condition, crystalline phase, average particle size, the semiquantitatively Cl^- and Br^- contents, surface area, and band gap for nanocrystalline TiO_2 materials. The crystalline phase of each sample was determined by powder XRD, and the corresponding diffraction patterns are shown in Figure 1. As the amount of HBr increases (from A−G), the phase changes from pure anatase (A and B), mixed anatase/rutile (C), pure rutile (D), mixed rutile/brookite (E), mixed anatase/rutile/brookite (F), and pure rutile (G).

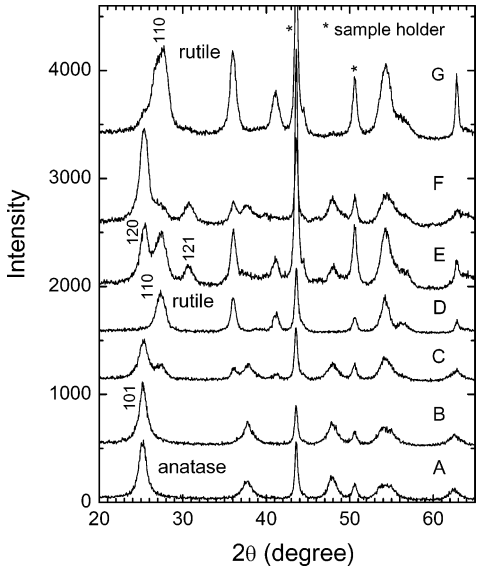

Figure 1. Powder XRD patterns of TiO_2 materials made by hydrothermal synthesis at 100 °C for 1 day from 2 mL of $TiCl_4$ and mixed ethanol−HBr system with varying amounts of HBr. Synthesis composition for each sample is shown in Table 1.

The semiquantitative phase composition of each sample with mixed anatase/rutile or mixed rutile/brookite was determined based on the relative peak intensities of anatase (101), rutile (110), and brookite (120) (the highest intensity peak for each pure phase). For the mixed anatase/rutile/brookite phases, due to the overlap of the highest intensity peak for anatase (101) and brookite (120), the weight percentage of anatase, rutile, and brookite was calculated from the integrated intensities of anatase (101), rutile (110), and brookite (121) peaks according to Zhang and Banfield.[19] The average

(15) Kortum, G. *Reflectances Spectroscopy*; Springer: New York, 1969.
(16) Domen, K.; Naito, S.; Onishi, T.; Tamaru, K.; Soma, M. *J. Phys. Chem.* **1982**, *86*, 3657.
(17) Sayama, K.; Arakawa, H. *J. Chem. Soc., Faraday Trans.* **1997**, *93*, 1647. Arakawa, H.; Sayama, K. *Catal. Surv. Jpn.* **2000**, *4*, 75.
(18) Kraeutler, B.; Bard, A. J. *J. Am. Chem. Soc.* **1978**, *100*, 4317.
(19) Zhang, H.; Banfield, J. F. *J. Phys. Chem. B* **2000**, *104*, 3481.

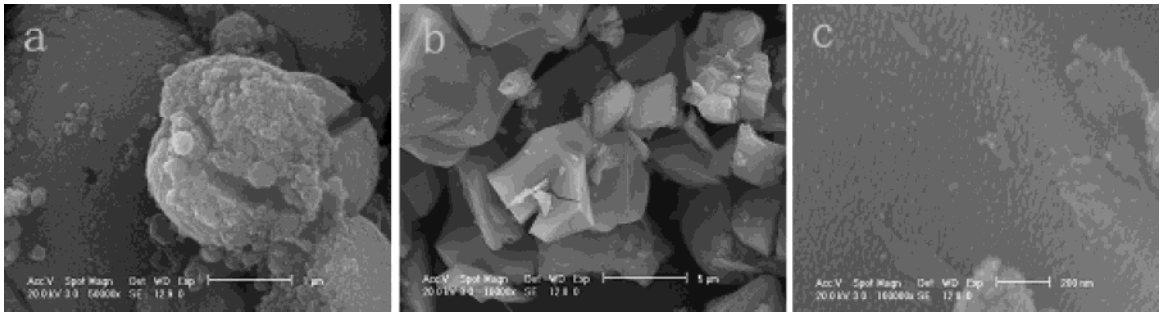

Figure 2. SEM images for rutile TiO_2 materials: (a) sample D; (b) and (c) sample G.

particle size was estimated by applying the Scherrer formula on the anatase (101), rutile (110), or brookite (121) diffraction peaks. An average size of around 10−12 nm was obtained for samples A−F and about 6 nm for G.

TiO_2 exists in three naturally occurring polymorphs: anatase, rutile, and brookite. Each structure exhibits different physical properties and has different applications. The results presented here clearly show for the first time that the phase and the phase composition of TiO_2 can be controlled by simply varying the amount of HBr in the synthesis solution, making it extremely useful to the systematic study of the photocatalytic activity of TiO_2.

N_2 adsorption measurements show that all samples except sample G are mesoporous with pore size of 3−4 nm, pore volume of 0.1−0.2 cm^3/g, and high surface area of 110−170 m^2/g. Sample G was prepared under very strong acidity and somehow has a low surface area of 49 m^2/g. Interestingly, the powder XRD shows that G has a smaller particle size than the other samples. Thus, higher surface area would have been expected from G. SEM pictures show that very fine particles pack densely for G, and all other samples have similar fine particulate morphology. Figure 2 shows the typical SEM images for two pure rutile phase samples, samples D and G, prepared under different acidity. The particle size obtained from the SEM image is consistent with that from XRD analyses. EDX analysis indicates that sample A contains Cl^- from the Ti source $TiCl_4$, and all other samples contain Br^- and Cl^-. The semiquantitatively atomic ratios of Br^- and Cl^- from EDX for the materials are indicated in Table 1. With increasing HBr amount in the starting system, Br^- doping amount increases while Cl^- doping decreases from sample A to D.

3.2. UV−Visible Reflectance Spectroscopy. Optical absorption spectra of the doped TiO_2 materials are shown in Figure 3. The absorption edge of the doped TiO_2 occurs at ca. 410−425 nm, and the band-gap energy is estimated to be about 2.95 eV for samples A and C, 3.0 for B, and 2.85 eV for D, which are smaller than 3.2−3.3 eV for nondoped anatase and 3.0−3.1 eV for nondoped rutile TiO_2.[20] Thus, Cl^- or Br^- and Cl^- doping for oxygen in TiO_2 causes the absorption edge of TiO_2 to shift to the lower energy region, similar to N, C, F, or S doping in TiO_2.

3.3. Photocatalytic Activity. Among the three main polymorphs, anatase TiO_2 is believed to exhibit the highest photocatalytic activity; thus, we choose several

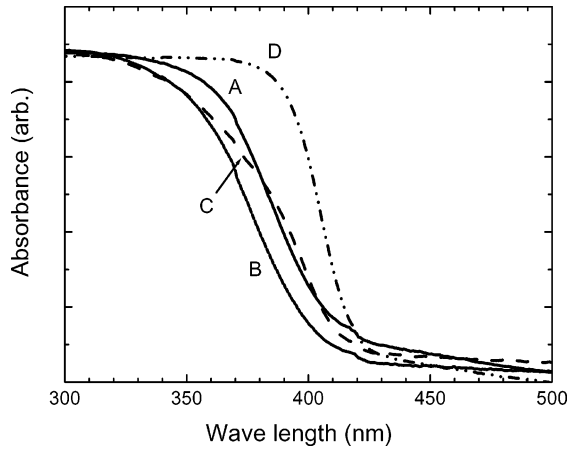

Figure 3. UV−visible reflectance spectra for doped TiO_2 materials: (A) Cl-doped anatase; (B) Br- and Cl-doped anatase; (C) Br- and Cl-doped 70% anatase and 30% rutile; (D) Br- and Cl-doped rutile.

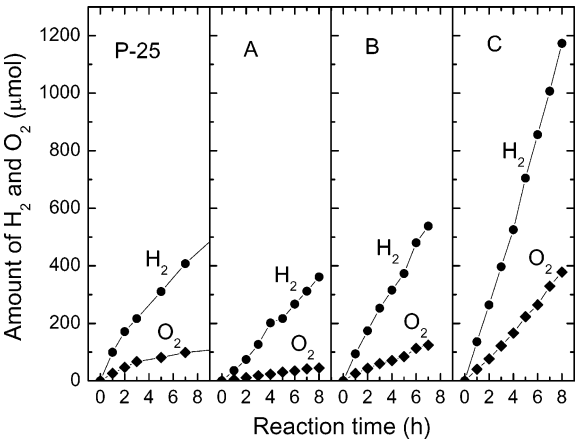

Figure 4. H_2 and O_2 evolution from an aqueous Na_2CO_3 solution over Pt-loaded TiO_2 materials compared with P-25: (A) Cl-doped anatase; (B) Br- and Cl-doped anatase; (C) Br- and Cl-doped 70% anatase and 30% rutile.

samples to measure the water splitting. Figure 4 shows the H_2 and O_2 evolution from Na_2CO_3 aqueous solution over some Pt-loaded TiO_2 materials under UV light. To investigate the stability of the catalysts, the photocatalytic reaction for each sample was carried out three times. The evolution rates of H_2 and O_2 were constant in every run. The ratio of H_2 to O_2 is above stoichiometric (H_2:O_2 = 2:1). The reason for less oxygen evolution could be the result of absorbed oxygen on the surface of the photocatalyst under UV irradiation.[20] It is clear that Cl^--doped anatase (sample A) has lower activity, but Br^- and Cl^- co-doped anatase TiO_2 (B) have

(20) Linsebigler, A. L.; Lu, G.; Yates, J. T., Jr. *Chem. Rev.* **1995**, *95*, 735.

similar activity to P-25. Co-doped 70% anatase and 30% rutile TiO_2 (C) has higher photocatalytic activity for water splitting than P-25. The rate of H_2 evolution for sample C is about 140 μmol/h, about twice that of P-25 (65 μmol/h) and sample B (75 μmol/h) and 3 times that of Cl^--doped anatase (A, 45 μmol/h). The higher activities for C than B are probably due to the presence of rutile phase in C. It is widely accepted that the mixed phases of the same semiconductor is beneficial in reducing the recombination of photogenerated electrons and holes and in enhancing photocatalytic activity.[21,22] For example, the high activity of standard P-25 is partially due to its composite nature consisting of 80% anatase and 20% rutile with a BET surface area of 50 m^2/g. The photocatalytic activity may be largely dependent on crystallinity, particle size, and crystal structure. From XRD, SEM, and N_2 adsorption measurement, the samples A, B, and C have almost the same particle size and surface area. Thus, it appears that Br^- and Cl^- co-doping for oxygen in TiO_2 enhances the photocatalytic activity for water splitting into H_2 and O_2. Since P-25 is considered as an excellent photocatalyst, 100% enhancement is certainly significant for water splitting.

4. Conclusions

Br^- and Cl^- co-doping TiO_2 nanoparticles with pure anatase, mixed anatase/rutile, pure rutile, mixed rutile/brookite, and mixed anatase/rutile/brookite phases have been prepared. Br^- and Cl^- co-doping narrows the band gap of TiO_2 and enhances the photocatalytic activity for H_2 and O_2 production in Na_2CO_3 aqueous solution under ultraviolet light. It is also possible that the Br^-- or Cl^--doping could lead to other transition-metal-based new visible light-driven photocatalysts.

Acknowledgment. We acknowledge the financial support from Riverside Public Utilities, California Energy Commission, and UC-SMART.

CM035090W

(21) Abe, R.; Sayama, K.; Domen, K.; Arakawa, H. *Chem. Phys. Lett.* **2001**, *344*, 339.
(22) Ohno, T.; Tokieda, K.; Higashida, S.; Matsumura, M. *Appl. Catal.* **2003**, *244*, 383.
(23) Tahiri, H.; Serpone, N.; LevanMao, R. *J. Photochem. Photobiol., A.* **1996**, *93*, 199.
(24) Fernandez-Ibanez, P.; de las Nieves, F. J.; Malato, S. *J. Colloid. Interface Sci.* **2000**, *227*, 510.